Journal of
Mechanics of
Materials and Structures

ANALYSIS OF PULL-IN INSTABILITY
OF ELECTROSTATICALLY ACTUATED CARBON NANOTUBES
USING THE HOMOTOPY PERTURBATION METHOD

Mir Masoud Seyyed Fakhrabadi, Abbas Rastgoo and Mohammad Taghi Ahmadian

msp

▪msp

ANALYSIS OF PULL-IN INSTABILITY
OF ELECTROSTATICALLY ACTUATED CARBON NANOTUBES
USING THE HOMOTOPY PERTURBATION METHOD

MIR MASOUD SEYYED FAKHRABADI, ABBAS RASTGOO AND MOHAMMAD TAGHI AHMADIAN

This paper analyzes the deflection and pull-in behaviors of cantilever and doubly clamped carbon nanotubes (CNTs) under electrostatic actuation using the homotopy perturbation method. The effects of electrostatic force and interatomic interactions on the deflection and pull-in instabilities of CNTs with different lengths, diameters, and boundary conditions are investigated in detail. The results reveal that larger diameters and shorter lengths result in higher pull-in voltages. Moreover, CNTs with doubly clamped boundary conditions, in comparison with cantilever boundary conditions, are more resistant to pull-in.

1. Introduction

Research into micro- and nanoelectromechanical systems (MEMS/NEMS) has experienced tremendous growth in recent years. The main motivations for scientists to conduct research in these fields are their combined electrical and mechanical properties, which result in simpler structures in electrical systems. This can be utilized in different electronic circuits, communication devices, and in aerospace applications such as sensors, actuators, resonators, capacitors, switches, etc. [Mojahedi et al. 2011; Kahrobaiyan et al. 2011; Darvishian et al. 2012; Moeenfard and Ahmadian 2012; Moeenfard et al. 2012; Rahaeifard et al. 2012]. MEMS and NEMS are, in general, mechanical devices such as micro/nanobeams, shells, plates, or other similar structures sensed or actuated electrically. Electrothermal, piezoelectric, and electrostatic systems are the most common types of actuation systems applied in the field of MEMS and NEMS [Ansola et al. 2012; Tayyaba et al. 2012; Zand 2012]. However, in nanoscale applications, electrostatic actuation is more frequently used and applicable.

Krylov et al. [2005] showed that parametric actuation of microstructure has stabilizing effects. They proposed that using this technique would result in higher pull-in voltages. They utilized the Hill and Mathieu equations to analyze the parametric actuation of these structures and verified the outcomes with experimental data. In the system considered in their article, a microbeam was attached to the ground plate while embedded between two positive electrodes. The electrical potential difference between the microbeam and electrodes causes it to deflect towards the fixed electrode with higher voltage. In another study, Zhang and Zhao [2006] studied the pull-in behaviors of microstructures under electrostatic actuation using numerical and analytical techniques. They applied a one-DOF model of the microbeams and analyzed the governing equations via Taylor expansion.

Batra et al. [2008] applied a reduced-order method to study the behaviors of rectangular and circular microplates in the presence of electrostatic actuation and Casimir effects. They used the nonlinear von Karman model to formulate the governing equations and presented the pull-in voltages for microstructures with different dimensions. Pirbodaghi et al. [2009] and Mojahedi et al. [2010] studied the static and dynamic behaviors of microbeams using the homotopy perturbation method. In the static case, the behaviors of the microbeams under electrostatic actuation were analyzed and pull-in voltages for different parameters were reported [Pirbodaghi et al. 2009]. For the dynamic case, the natural frequencies of microbeams under two cantilever and doubly clamped boundary conditions were extracted [Mojahedi et al. 2010].

Rezazadeh et al. [2011] studied the static and dynamic behaviors of microbeams using a one-DOF model and presented some equations to obtain the static and dynamic pull-in voltages. These relations could be used to estimate pull-in voltages without requiring solving the governing partial differential equations. Moghimi Zand et al. [2009] investigated the behaviors of microbeams under suddenly applied voltages and analyzed the effects of increments in voltages, residual stresses, and fringing fields using the homotopy perturbation method. Jia et al. [2011] studied the behaviors of microbeams in the presence of electrostatic actuation and Casimir forces considering geometrically nonlinear vibration on the pull-in phenomena.

The papers above show the depth of interest in MEMS; we now mention a few studies of NEMS. Technological progress has gone hand in hand with a decrease in the size of electrical devices embedded in electrical appliances such as cell phones, cameras, micro- and nanorobots, etc. Hence nanosystems have also been the object of intense attention. Nanobeams and nanotubes are the first choices one may consider in NEMS applications.

Ramezani et al. [2008a] studied the effects of Casimir forces on the electrostatic behaviors of nanobeams. They applied a Green's function to transform the nonlinear governing equation to an integrodifferential equation and considered an appropriate shape function to obtain an analytic relation for the deflection of nanobeams actuated electrostatically. They also investigated in [Ramezani et al. 2008b] the effects of van der Waals (vdW) force on the properties mentioned.

Abadyan et al. [2010] applied the homotopy perturbation method to investigate the effects of Casimir force on the pull-in instability of cantilever nanobeams. They studied the static pull-in of nanobeams using this method and compared the results with those reported in the literature. Soroush et al. [2010] studied the effects of Casimir and vdW forces on the pull-in instability of cantilevered nanobeams. They applied the Adomian decomposition method to obtain an analytical solution based on the distributed parameter model. In addition, Koochi et al. [2012] investigated the influence of surface effects including residual surface stress and surface elasticity on the size-dependent instability of nanobeams in the presence of Casimir forces using the Adomian decomposition technique.

There are fewer papers on electrostatically actuated nanobeams than there are for microbeams. However, electrostatic actuation of carbon nanotubes (CNTs), even in comparison with nanobeams, has not been investigated comprehensively and obviously deserves more attention.

Dequesnes et al. [2002] may be the first researchers to study the static pull-in behaviors of CNTs under electrostatic actuation and vdW force. They applied a one-DOF model in their research, which was a simplification and might have some deviation from the real systems. Ke and Espinosa [2005; 2005] presented two papers regarding CNT-based NEMS. The first focused on the quality of charge distribution, and the second was about stretching effects on doubly clamped CNTs. In addition, Ouakad and Younis

[2010] studied the nonlinear dynamic behaviors of CNTs under electrostatic actuation and presented the frequency response of these systems given different applied voltages.

In this paper, we study static and dynamic behaviors as well as pull-in instability of CNTs with different geometries and boundary conditions under electrostatic actuation. The governing equations, as presented in the following section, are nonlinear and may not be solved analytically by the typical approaches. Hence, either numerical or some special analytic or semianalytic techniques should be applied to analyze these phenomena in CNTs. He's homotopy perturbation method is applied in this paper. This technique has some advantages over other common methods, such as fast and safe convergence. Moreover, it doesn't need to discretize the space and time domains, unlike many other numerical techniques. Two other advantages are that less computational cost is needed, and solving nonlinear discrete systems of differential equations is not required.

2. Definition of the problem

This section defines the system under consideration and formulates governing equations. It also covers the description of the homotopy perturbation method that is to be applied to solve the resultant equations.

As shown in Figure 1, suppose that a CNT is suspended over some graphene sheets with an initial gap of G_0 (state 1 in Figure 1). With the CNT as the positive electrode and the graphene sheets as the negative electrode (ground plate), an electrical potential difference (V) is applied. The charge distributions over the electrodes create an attractive force between the positive and negative electrodes. This force along with the interatomic force between the electrodes leads to a deflection of the CNT towards the ground plate (state 2 in Figure 1). The deflection value ($w = w(x)$ in Figure 1) corresponds to the applied voltage up to where the elastic force of the CNT cannot tolerate the attractive force resulting from the applied voltage and the interatomic forces. Hence, it then drops suddenly on the ground plate. This phenomenon is called pull-in instability and the corresponding voltage is the pull-in voltage. Pull-in instability usually occurs at a deflection of about one third to one half of the gap distance.

In the following, formulation of the static and dynamic behaviors and pull-in instabilities of CNTs are conducted. The governing equations and solution methods of each item are presented.

2.1. *Static pull-in.* The deflation of a doubly clamped CNT actuated using a step DC voltage can be obtained from
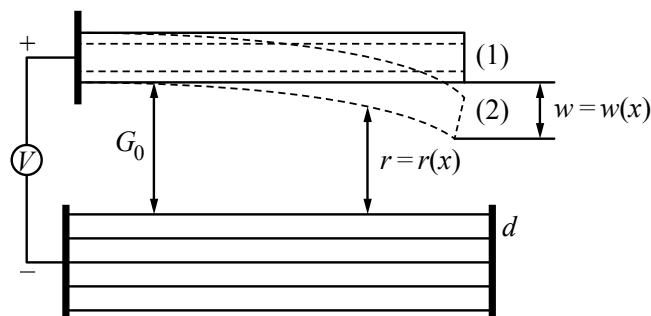

Figure 1. Deflection of a CNT under electrostatic actuation.

$$EI\frac{d^4w}{dx^4} - \left(\frac{EA}{2L}\int_0^L \left(\frac{dw}{dx}\right)^2 dx\right)\frac{d^2w}{dx^2} = q_{\text{elec}} + q_{\text{vdW}}, \tag{1}$$

where, in the left-hand side of the equation, E is the elastic modulus, I is the moment of inertia, w is the deflection, x is the axial coordinate, A is the cross sectional area, and L is the length of the CNT. The right-hand side of the equation includes q_{elec} and q_{vdW}, which are the distributed forces applied by the electrostatic voltage and vdW interatomic effects, respectively.

The boundary conditions corresponding to the cantilever and doubly clamped CNTs are presented in (2) and (3). The second term in the left-hand side of (1) is due to midplane stretching and equals zero for the cantilevered CNTs:

$$\frac{\partial w(0,t)}{\partial x} = w(0,t) = \frac{\partial w(L,t)}{\partial x} = w(L,t) = 0, \tag{2}$$

$$\frac{\partial w(0,t)}{\partial x} = w(0,t) = \frac{\partial^2 w(L,t)}{\partial x^2} = \frac{\partial^3 w(L,t)}{\partial x^3} = 0. \tag{3}$$

The maximum deflections of the cantilever and doubly clamped CNTs are, respectively, at the tip and longitudinal center. Thus, the critical points to study the deflection of CNTs under the boundary conditions mentioned are these points.

The electrostatic force is formulated as [Dequesnes et al. 2002]

$$q_{\text{elec}}cl = \frac{\pi\epsilon_0 V^2}{\sqrt{(G_0 - w)(G_0 - w + 2R)}\text{arccosh}^2(1 + (G_0 - w)/R)}, \tag{4}$$

where ϵ_0 is the electrical permittivity, V the voltage, R the radius of the CNT, and G_0 the initial gap.

The vdW force of the system can be formulated as [Dequesnes et al. 2002]

$$q_{\text{vdW}} = \frac{\pi^2 c_6 \sigma^2}{2}\sum_{n=1}^{N_G} \frac{R\left(\begin{array}{c}8(G_0 + (n-1)d - w)^4 + 32(G_0 + (n-1)d - w)^3 R \\ + 72(G_0 + (n-1)d - w)^2 R^2 + 80(G_0 + (n-1)d - w)R^3 + 35R^4\end{array}\right)}{(G_0 + (n-1)d - w)^{9/2}(G_0 + (n-1)d - w + 2R)^{9/2}}, \tag{5}$$

where c_6 and σ^2 are Lennard-Jones potential parameters describing the vdW force and N_G represents the number of graphene sheets.

In order to solve the governing equations of the deflection of the CNTs under electrostatic actuation, it is better to normalize the equations by considering the following nondimensional parameters:

$$\bar{w} = \frac{w}{G_0}, \quad \bar{x} = \frac{x}{L}, \quad \bar{R} = \frac{R}{G_0}, \quad \bar{d} = \frac{d}{G_0}. \tag{6}$$

Replacing the above parameters into the terms of (1) and (5), we have

$$\frac{\partial^4 \bar{w}}{\partial \bar{x}^4} - \alpha_1 \frac{\partial^2 \bar{w}}{\partial \bar{x}^2} + \beta_1 \frac{\partial^2 \bar{w}}{\partial \bar{t}^2} + \gamma_1 \frac{\partial \bar{w}}{\partial \bar{t}} = \bar{q}_{\text{elec}}(\bar{w}) + \bar{q}_{\text{vdW}}(\bar{w}), \tag{7}$$

where

$$\alpha_1 = \left[\left(\alpha \int_0^1 \left(\frac{d\bar{w}}{d\bar{x}}\right)^2 d\bar{x}\right)\right];$$

here $\alpha = AG_0^2/(2I)$ for doubly clamped boundary conditions, $\alpha = 0$ for cantilever boundary conditions,

and

$$\beta_1 = m_c \frac{L^4}{EIt^{*2}}, \quad \gamma_1 = \frac{cL^4}{EIt^*}, \quad \beta = \frac{\pi \epsilon_0 L^4}{EIG_0^2},$$

$$\bar{q}_{\text{elec}}(\bar{w}) = \frac{\beta V^2}{\sqrt{(1-\bar{w})(1-\bar{w}+2\bar{R})}\text{arccosh}^2(1+(1-\bar{w})/\bar{R})}, \quad \gamma = \frac{\pi^2 c_6 \sigma^2 L^4}{2EIG_0^5},$$

$$\bar{q}_{\text{vdW}}(\bar{w}) = \gamma \sum_{n=1}^{N_G} \frac{\bar{R}\left(\begin{array}{l} 8(1+(n-1)\bar{d}-\bar{w})^4 + 32(1+(n-1)\bar{d}-\bar{w})^3\bar{R} \\ +72(1+(n-1)\bar{d}-\bar{w})^2\bar{R}^2 + 80(1+(n-1)\bar{d}-\bar{w})\bar{R}^3 + 35\bar{R}^4 \end{array}\right)}{(1+(n-1)\bar{d}-\bar{w})^{9/2}(1+(n-1)\bar{d}-\bar{w}+2\bar{R})^{9/2}}. \tag{8}$$

Expansion theory is applied at this stage to solve the governing equations. Suppose that deflection can be formulated as

$$\bar{w} = \sum_{i=1}^{n} a_i \phi_i(x), \tag{9}$$

where a_i are the coefficients and $\phi_i(x)$ are the shape modes. The shape modes corresponding to the cantilever and doubly clamped boundary conditions are presented in (10) and (11), respectively [Mojahedi et al. 2010]:

$$\phi(x) = \cosh \mu \bar{x} - \cos \mu \bar{x} - \frac{\cosh \mu + \cos \mu}{\sinh \mu + \sin \mu}(\sinh \mu \bar{x} - \sin \mu \bar{x}), \quad \mu_{1\text{st}} = 1.875, \tag{10}$$

$$\phi(x) = \cosh \lambda \bar{x} - \cos \lambda \bar{x} - \frac{\cosh \lambda - \cos \lambda}{\sinh \lambda - \sin \lambda}(\sinh \lambda \bar{x} - \sin \lambda \bar{x}), \quad \lambda_{1\text{st}} = 4.73. \tag{11}$$

For static deflection of the CNT, the first mode is enough. Hence, (9) can be written as

$$\bar{w} = a\phi(\bar{x}). \tag{12}$$

By substituting (12) into (7), we have

$$a\frac{d^4\phi(\bar{x})}{d\bar{x}^4} - \alpha a^3 \phi''(\bar{x}) \int_0^1 \phi'(\bar{x})^2 \, d\bar{x} = \bar{q}_{\text{elec}}(a\phi(\bar{x})) + \bar{q}_{\text{vdW}}(a\phi(\bar{x})). \tag{13}$$

The Galerkin method is applied to (13) to solve it. By multiplying all of the terms by $\phi(\bar{x})$ and integrating over the domain, we can write

$$k_1 a + k_2 a^3 - \int_0^1 \bar{q}_{\text{elec}}(a\phi(\bar{x}))\phi(\bar{x}) \, d\bar{x} - \int_0^1 \bar{q}_{\text{vdW}}(a\phi(\bar{x}))\phi(\bar{x}) \, d\bar{x} = 0, \tag{14}$$

where

$$k_{1s} = \int_0^1 \left(\frac{d^2\phi(\bar{x})}{d\bar{x}^2}\right)^2 d\bar{x}, \quad k_{2s} = \alpha \left(\int_0^1 \phi'(\bar{x})^2 \, d\bar{x}\right)^2. \tag{15}$$

Equation (14) is the final governing formula for analyzing the static deflection of the CNT under electrostatic actuation. It should be solved to obtain the deflection of the CNT under different applied voltages as well as the pull-in voltage.

2.1.1. *The homotopy perturbation method for solving static deflection.* Here we are going to solve a nonlinear differential equation with the boundary conditions given as [Mojahedi et al. 2010]

$$A(u) - f(r) = 0, \quad r \in \Omega, \tag{16a}$$

$$B\left(u, \frac{\partial u}{\partial n}\right) = 0, \quad r \in \Gamma, \tag{16b}$$

where A denotes a general nonlinear operator, u an unknown function, $f(r)$ a given function of the variable r, Ω the problem domain, B a given function for the boundaries, n a given direction, and Γ the domain boundaries. The general nonlinear operator may be divided into linear, $L(u)$, and nonlinear, $N(u)$, parts. The main relation of the homotopy perturbation technique is

$$H(a, p) = L(a) - L(\bar{a}) + p(N(a) + L(\bar{a})) = 0, \tag{17}$$

where $\bar{a}$ is the initial guess satisfying the boundary conditions and a denotes the solution of the problem, which can be considered as

$$a = a_0 + pa_1 + p^2 a_2 + p^3 a_3 + p^4 a_4 + p^5 a_5 + \cdots. \tag{18}$$

Also, $p \in [0, 1]$ is an embedding parameter. A p value of zero causes a to correspond to the initial guess and a p value of one causes a to converge to the solution of the problem. In addition, $N(a)$ can be expanded in Taylor series as [Mojahedi et al. 2010]

$$\begin{aligned}
N(a) = N(a_0) &+ N'(a_0)(pa_1 + p^2 a_2 + p^3 a_3 + p^4 a_4 + p^5 a_5) \\
&+ \frac{N''(a_0)}{2!}(pa_1 + p^2 a_2 + p^3 a_3 + p^4 a_4 + p^5 a_5)^2 \\
&+ \frac{N'''(a_0)}{3!}(pa_1 + p^2 a_2 + p^3 a_3 + p^4 a_4 + p^5 a_5)^3 \\
&+ \frac{N^{(4)}(a_0)}{4!}(pa_1 + p^2 a_2 + p^3 a_3 + p^4 a_4 + p^5 a_5)^4.
\end{aligned} \tag{19}$$

Substituting (19) in (17), the coefficients of p^i, $i = 1, \ldots, 5$ are obtained as

$$\begin{aligned}
&p^0 : L(a_0) - L(\bar{a}) = 0, \\
&p^1 : L(a_1) + N(a_0) + L(\bar{a}) = 0, \\
&p^2 : L(a_2) + a_1 N'(a_0) = 0, \\
&p^3 : L(a_3) + a_2 N'(a_0) + a_1 \frac{N''(a_0)}{2!} = 0, \\
&p^4 : L(a_4) + a_3 N'(a_0) + \frac{2a_1 a_2}{2!} N''(a_0) + \frac{a_1^3}{3!} N'''(a_0) = 0, \\
&p^5 : L(a_5) + a_4 N'(a_0) + \frac{2a_1 a_3 + a_2^2}{2!} N''(a_0) + \frac{3a_1^2 a_2}{3!} N'''(a_0) + \frac{a_1^4}{4!} N^{(4)}(a_0) = 0.
\end{aligned} \tag{20}$$

For the current problem, according to (14), the linear and nonlinear parts are selected as

$$L(a) = k_{1s}a, \tag{21a}$$

$$N(a) = k_{2s}a^3 - \int_0^1 \bar{q}_{\text{elec}}(a\phi(\bar{x}))\phi(\bar{x})\,d\bar{x} - \int_0^1 \bar{q}_{\text{vdW}}(a\phi(\bar{x}))\phi(\bar{x})\,d\bar{x}. \tag{21b}$$

The above equations should be solved using the described technique in order to obtain the deflection and pull-in voltages of CNTs actuated electrostatically.

2.2. Dynamic pull-in. The deflation of the doubly clamped CNT applied a step DC voltage can be obtained from

$$EI\frac{\partial^4 w}{\partial x^4} - \left(\frac{EA}{2L}\int_0^L \left(\frac{\partial w}{\partial x}\right)^2 dx\right)\frac{\partial^2 w}{\partial x^2} + m\frac{\partial^2 w}{\partial t^2} = q_{\text{elec}} + q_{\text{vdW}}, \tag{22}$$

where m and t are, respectively, the mass of the CNT per length and time. Similarly to the static case, the second term equals zero for the cantilevered CNTs. The other variables were all introduced before. The first step in solving the above equation is nondimensionalization. The nondimensional parameters introduced in (6) and $\bar{t} = t/\sqrt{mL^4/EI}$ are applied for this purpose. The nondimensional form of (22) is obtained as

$$\frac{\partial^4 \bar{w}}{\partial \bar{x}^4} - \left(\alpha \int_0^1 \left(\frac{\partial \bar{w}}{\partial \bar{x}}\right)^2 d\bar{x}\right)\frac{\partial^2 \bar{w}}{\partial \bar{x}^2} + \eta\frac{\partial^2 \bar{w}}{\partial \bar{t}^2} = \bar{q}_{\text{elec}}(\bar{w}) + \bar{q}_{\text{vdW}}(\bar{w}), \tag{23}$$

where η equals

$$\frac{mL^4}{EIG_0} \Bigg/ \frac{mL^4}{EIG_0} = 1,$$

and other variables including α, q_{elec}, and q_{vdW} were introduced in previous equations.

The Taylor expansions of the right-hand terms of (23) are

$$\bar{q}_{\text{elec}}(\bar{w}) = \sum_{i=0}^n A_i w^i, \tag{24}$$

$$\bar{q}_{\text{vdW}}(\bar{w}) = \sum_{i=0}^n B_i w^i. \tag{25}$$

The coefficients A_i and B_i are obtained from the derivative terms of the Taylor expansions. We consider five terms for the expansions; the two first terms of $\bar{q}_{\text{elec}}(\bar{w})$ and $\bar{q}_{\text{vdW}}(\bar{w})$ are presented in (26) and (27). The others are not reported here for brevity. Our calculations show that considering more than five terms does not add any accuracy to the results. The first two terms are:

$$A_0 = \frac{\beta V^2}{\sqrt{1+2R}\,\text{arccosh}^2((R+1)/R)},$$

$$A_1 = \frac{2\beta V^2}{(1+2R)\text{arccosh}^3((R+1)/R)} + \frac{\frac{1}{2}\frac{\beta V^2}{(1+2R)^{3/2}} + \frac{1}{2}\frac{\beta V^2}{\sqrt{1+2R}}}{\text{arccosh}^2((R+1)/R)}, \tag{26}$$

and

$$B_0 = \gamma \sum_{n=1}^{N_G} \frac{\bar{R}\left(\begin{array}{c}8(1+(n-1)\bar{d})^4 + 32(1+(n-1)\bar{d})^3\bar{R} \\ +72(1+(n-1)\bar{d})^2\bar{R}^2 + 80(1+(n-1)\bar{d})\bar{R}^3 + 35\bar{R}^4\end{array}\right)}{(1+(n-1)\bar{d})^{9/2}(1+(n-1)\bar{d}+2\bar{R})^{9/2}},$$

$$B_1 = \gamma \sum_{n=1}^{N_G} \left[\frac{9}{2} \frac{\bar{R}\left(\begin{array}{c}8(1+(n-1)\bar{d})^4 + 32(1+(n-1)\bar{d})^3\bar{R} \\ +72(1+(n-1)\bar{d})^2\bar{R}^2 + 80(1+(n-1)\bar{d})\bar{R}^3 + 35\bar{R}^4\end{array}\right)}{(1+(n-1)\bar{d})^{9/2}(1+(n-1)\bar{d}+2\bar{R})^{11/2}} \right.$$

$$\left. + \frac{1}{(1+(n-1)\bar{d}+2\bar{R})^{\frac{9}{2}}} \left(\begin{array}{c} \dfrac{9}{2}\dfrac{\bar{R}\left(\begin{array}{c}8(1+(n-1)\bar{d})^4+32(1+(n-1)\bar{d})^3\bar{R} \\ +72(1+(n-1)\bar{d})^2\bar{R}^2+80(1+(n-1)\bar{d})\bar{R}^3+35\bar{R}^4\end{array}\right)}{(1+(n-1)\bar{d})^{11/2}} \\[2ex] + \dfrac{\bar{R}(32((1+(n-1)\bar{d})(-2-2(n-1)\bar{d})-(1+(n-1)\bar{d})^2)\bar{R})}{(1+(n-1)\bar{d})^{9/2}} \\[2ex] + \dfrac{16(1+(n-1)\bar{d})^2(-2-2(n-1)\bar{d})-80\bar{R}^3+72(-2-2(n-1)\bar{d})\bar{R}^2}{(1+(n-1)\bar{d})^{9/2}} \end{array}\right) \right]. \tag{27}$$

The Taylor expansion applied at this stage is around $w = 0$. The results will show that the applied technique is in good agreement with previous studies, but it may have some inaccuracy for larger gaps. Suppose that $C_i = A_i + B_i$. Substituting (24), (25), and (28) into (23) and using the Galerkin method, we have the final governing equation in (29):

$$\bar{w} = \sum_{i=1}^{n} u_i(t)\phi_i(x), \tag{28}$$

$$k_{1d}\frac{d^2u(t)}{dt^2} + k_{2d}u(t) + k_{3d}u^3(t) = k_{4d} + k_{5d}u(t) + k_{6d}u^2(t) + k_{7d}u^3(t) + k_{8d}u^4(t) + k_{9d}u^5(t), \tag{29}$$

where

$$k_{1d} = \int_0^1 \eta\phi^2(x)\,dx, \qquad k_{2d} = \int_0^1 \left(\frac{d^2\phi(x)}{dx^2}\right)^2 dx, \qquad k_{3d} = \left[\int_0^1 \alpha\left(\frac{d\phi(x)}{dx}\right)^2 dx\right]^2,$$

$$k_{4d} = C_1\int_0^1 \phi(x)\,dx, \qquad k_{5d} = C_2\int_0^1 \phi^2(x)\,dx, \qquad k_{6d} = C_3\int_0^1 \phi^3(x)\,dx, \tag{30}$$

$$k_{7d} = C_4\int_0^1 \phi^4(x)\,dx, \qquad k_{8d} = C_5\int_0^1 \phi^5(x)\,dx, \qquad k_{9d} = C_5\int_0^1 \phi^6(x)\,dx.$$

2.2.1. *The homotopy perturbation method for solving dynamic pull-in.* In order to solve the governing equation of the dynamic behavior of CNTs under step DC voltage, the following technique is applied. Although the concepts are similar to the previous description in Section 2.1.1, the formulations are arranged a little differently. Suppose that the nonlinear differential equation to be solved is

$$R(u(t)) = 0, \tag{31}$$

where R is the nonlinear operator and $u(t)$ is the unknown function [Moghimi Zand and Ahmadian 2009]. Using $q \in [0, 1]$ as an embedding parameter, the homotopy function can be written as

$$H(\Phi, q) = (1 - q)L[\Phi(t, q) - u_0(t)] - qR[\Phi(t, q), \Omega(q)] = 0, \tag{32}$$

where $u_0(t)$ is the initial guess satisfying the boundary conditions, L is the nonzero auxiliary operator, and Ω is the frequency of the solution. This equation is similar to (17). As q increases from zero to one, $\Phi(t, q)$ changes from the initial guess $\Phi(t, 0) = u_0(t)$ to the exact solution $\Phi(t, 1) = u(t)$. Using Taylor expansion, $\Phi(t, q)$ can be expanded with respect to q as

$$\Phi(t, q) = \Phi(t, 0) + \lim_{n \to \infty} \sum_{j=1}^{n} \frac{1}{j!} \left. \frac{\partial^j \Phi(t, q)}{\partial q^j} \right|_{q=0} q^j = u_0(t) + \lim_{n \to \infty} \sum_{j=1}^{n} u_j(t) q^j, \tag{33}$$

where $u_j(t)$ is called the j-th order deformation derivative. Solving (33), we can write

$$(1 - q)L[\Phi(t, q) - u_0(t)] = qR[\Phi(t, q), \Omega(q)], \tag{34a}$$

$$\Phi(0, q) = 0, \quad \frac{d\Phi(0, q)}{dt} = 0. \tag{34b}$$

If $q = 0$, then (34a) turns to the following relation to obtain the zero-order deformation:

$$L[\Phi(t, 0) - u_0(t)] = 0. \tag{35}$$

Differentiating (34a) with respect to q and setting $q = 0$, the first-order deformation relation with zero initial conditions can be obtained:

$$L[u_1(t)] = qR[\Phi(t, q), \Omega(q)]\big|_{q=0}. \tag{36}$$

Taking the j-th order differential of (34a) and then setting $q = 0$ results in the j-th order deformation equation [Moghimi Zand and Ahmadian 2009]:

$$L[u_j(t) - \delta_j u_{j-1}(t)] = \frac{1}{(j-1)!} \left. \frac{\partial^{j-1} R[\Phi(t, q), \Omega(q)]}{\partial q^{j-1}} \right|_{q=0}, \tag{37}$$

where

$$\delta_j = \begin{cases} 0, & \text{if } j \leq 1, \\ 1, & \text{otherwise.} \end{cases} \tag{38}$$

Higher-order approximations of the exact solution can be achieved by solving (37).

At this stage, the homotopy perturbation method is applied to solve the governing equations of the CNT deflection and pull-in under step DC voltage. Using a new time scale $\tau = \omega t$, (30) can be rewritten as follows:

$$k_{1d}\omega^2 \frac{d^2u(\tau)}{d\tau^2} + k_{2d}u(\tau) + k_{3d}u^3(\tau) - k_{4d} - k_{5d}u(\tau) - k_{6d}u^2(\tau) - k_{7d}u^3(\tau) - k_{8d}u^4(\tau) - k_{9d}u^5(\tau) = 0. \tag{39}$$

The nonlinear and linear operators of (33) are defined as

$$R[\Phi(\tau, q), \Omega(q)] = k_{1d}\omega(q)^2 \frac{\partial^2 \Phi(\tau, q)}{\partial \tau^2} + k_{2d}\Phi(\tau, q) + k_{3d}\Phi(\tau, q)^3 - k_{4d}$$

$$- k_{5d}\Phi(\tau, q) - k_{6d}\Phi(\tau, q)^2 - k_{7d}\Phi(\tau, q)^3 - k_{8d}\Phi(\tau, q)^4 - k_{9d}\Phi(\tau, q)^5, \quad (40)$$

$$L[\Phi(t, q)] = \omega_0^2 \left(\frac{\partial^2 \Phi(t, q)}{\partial \tau^2} + \Phi(t, q) \right). \quad (41)$$

The initial guess for the system deflection is considered $u_0(\tau) = 0$. The first-order approximation is obtained by solving (36):

$$u_1(t) = \frac{k_4}{\omega_0^2}(1 - \cos(\tau)). \quad (42)$$

The governing equation of the undamped vibration of the CNT should be expressed based on the base functions

$$\cos(m\tau) = 0, \quad m = 1, 2, 3, \ldots. \quad (43)$$

Hence, in order to eliminate the secular terms in the j-th order approximation, the coefficients of $\cos(\tau)$ in the $(j-1)$-th order deformation equation should be set to zero. This fact results in an algebraic equation and its solution leads to ω_{j-2}. The second-order approximation is obtained from solving (37) as

$$u_2(\tau) = \frac{k_1 k_4 (1 + k_1)(1 - \cos(\tau))}{k_2 + k_5}, \quad \omega_0 = \frac{\sqrt{k_1(k_2 + k_5)}}{k_1}. \quad (44)$$

Successive solution of (37) for the higher-order approximations and setting $q = 1$ result in more-exact results according to

$$u(\tau) = \sum_{j=0}^{n+2} u_j(t), \quad \omega = \sum_{j=0}^{n} \omega_j. \quad (45)$$

3. Results and discussion

In this section, the results obtained from the above formulations are presented. The results cover the deflection of CNTs with different geometries and boundary conditions under electrostatic actuation in the presence of vdW effects as well as their pull-in voltages. The numerical values applied in the paper are presented in Table 1. They are fixed unless stated explicitly.

First of all, in order to verify the formulation and applied technique to solve the governing equations, we are going to compare some results of this paper with those reported in [Dequesnes et al. 2002]. Figure 2 illustrates the tip deflection of a cantilever and center-point deflection of a doubly clamped CNT studied in [ibid.] ($R_{\text{int}} = 6.65\,\text{A}$, $R_{\text{ext}} = 10\,\text{A}$, and $E = 1.2\,\text{TPa}$) versus voltage. The results obtained from the formulation presented in that paper are depicted in the same figures. The diagrams reveal good agreement between the results and confirm our formulation and applied solutions method. The inconsequential differences may be due to different solution techniques and various formulations. Duquesnes et al. considered a one-DOF model, while in this paper we consider a more real distributed model.

Parameter	Numerical value
Elastic modulus	1 TPa
Electric permittivity	$8.854 \times 10^{-12}\,\mathrm{C}^2/\mathrm{Nm}^2$
Gap distance	4 nm
Length	50 nm
Radius	6.785 A
Lennard-Jones (c_6)	$2.43 \times 10^{-78}\,\mathrm{Nm}^7$
Lennard-Jones (σ)	$1.14 \times 10^{29}\,\mathrm{m}^{-3}$

Table 1. Numerical values applied in the paper. For the parameters of the Lennard-Jones potential, see [Dequesnes et al. 2002].

As shown in Figure 2, the deflections of the CNTs increase with the voltage up to maximum values, and then suddenly drop on the ground plate. This phenomenon is called pull-in, and the corresponding voltage, as described before, is the pull-in voltage. The figures reveal that the vdW force decreases the pull-in voltage of the CNTs with both boundary conditions, but the effects are remarkably higher for the cantilevered CNTs. Hence, it has a very important role and cannot be disregarded in NEMS. There are several key points in the figures that we will discuss in detail. At zero voltage (the absence of electrostatic actuation), there is an initial deflection in the cantilevered CNTs. The deflection is the resulted of the vdW interaction between the CNT and substrate. Thus, the vdW force not only decreases the pull-in voltage but also applies an initial deflection to the system before any external actuation. However, this deflection is ignorable for the doubly clamped CNT due to its stiffer structure. Comparison between the two parts of Figure 2 reveals that the pull-in voltages of the doubly clamped CNTs are much larger than those of the cantilevered CNTs with same dimensions. This is also because of the weaker structures of the cantilevered CNTs in comparison with the doubly clamped CNTs. We now study the effects of variation in dimensions on the pull-in voltages of CNTs under cantilever and doubly clamped boundary conditions.
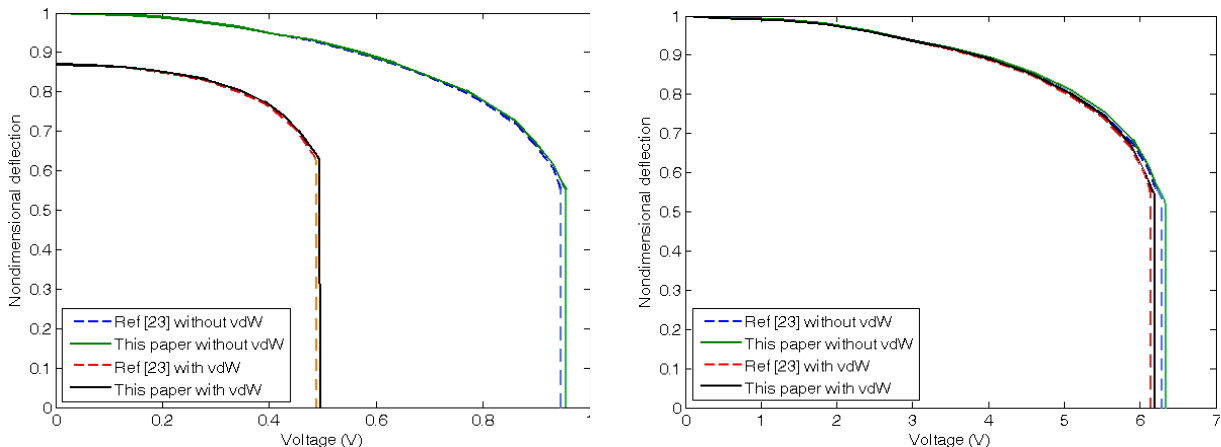
Figure 2. Deflection of CNTs with (left) cantilever and (right) doubly clamped boundary conditions under electrostatic actuation.

3.1. *Deflection of CNTs under static DC actuation.*   We next discuss the effects of changes in the dimensions of CNTs on the static electrostatic actuation under the boundary conditions mentioned. Figure 3 shows the pull-in voltages of the cantilevered and doubly clamped CNTs versus length. The figure reveals that with increasing length of the CNT, the pull-in occurs at smaller voltages. It is worth noting that the longer cantilevered CNTs may encounter pull-in instability only by the vdW interaction. This means that in the absence of electrostatic actuation, vdW forces can make the longer nanosystems pull in. For example, a cantilevered CNT with length of 60 nm and other characteristics the same as those mentioned in Table 1 pulls in only because of vdW interactions.

Figure 4 illustrates the pull-in voltages of the systems with various radii. The results reveal that CNTs with larger radii have higher pull-in voltages. Thus, they deflect harder than those with smaller radii because larger radii lead to stiffer CNTs.
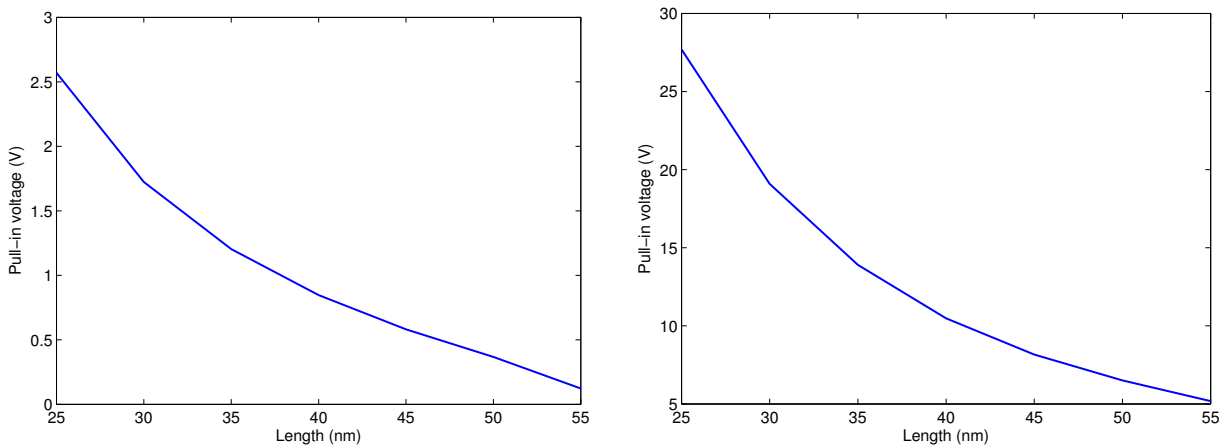
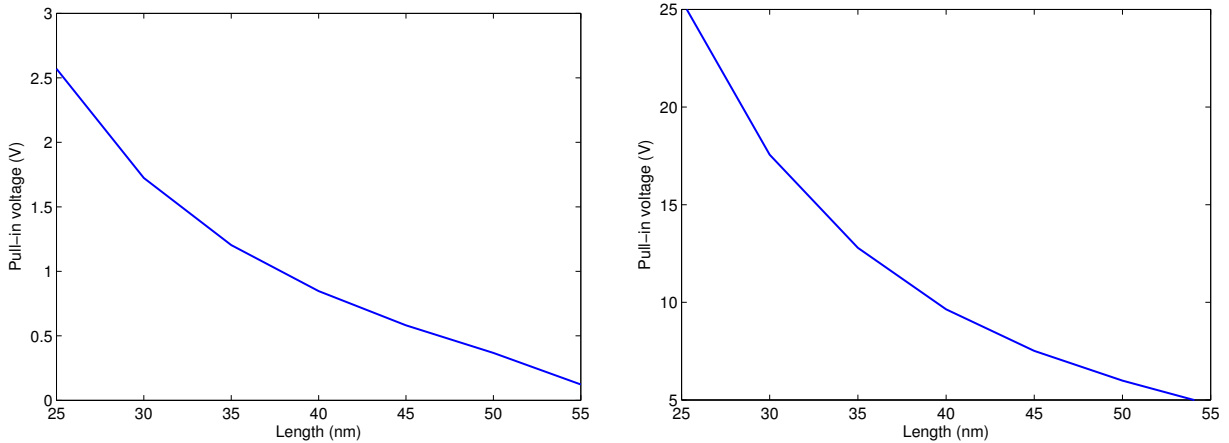**Figure 3.** Static pull-in voltages versus length of CNTs with (left) cantilever and (right) doubly clamped boundary conditions.
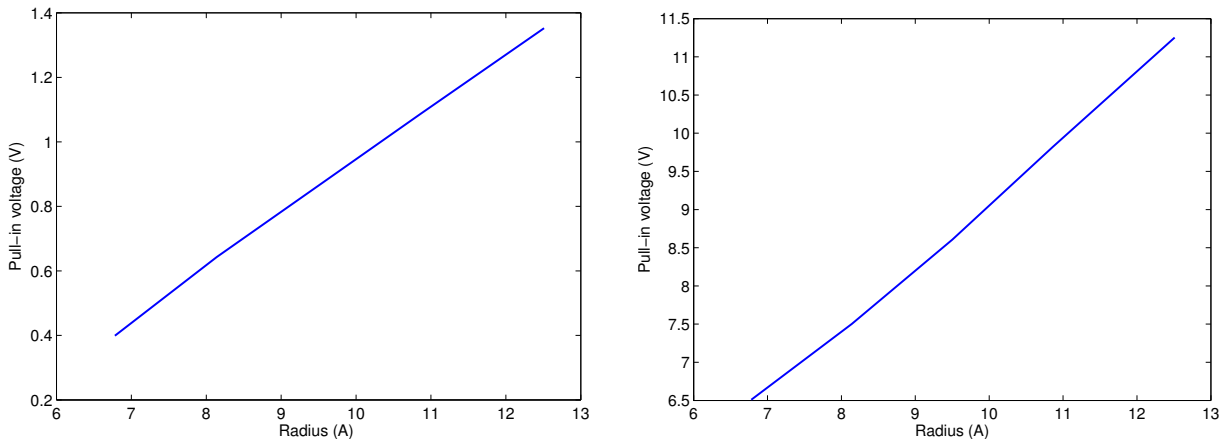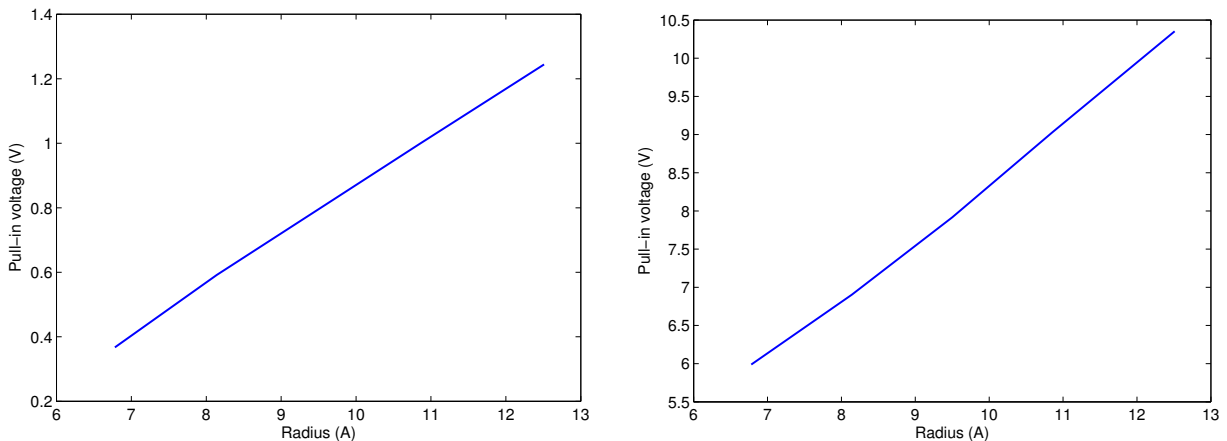

Figure 4. Static pull-in voltages versus radius of CNTs with (left) cantilever and (right) doubly clamped boundary conditions.
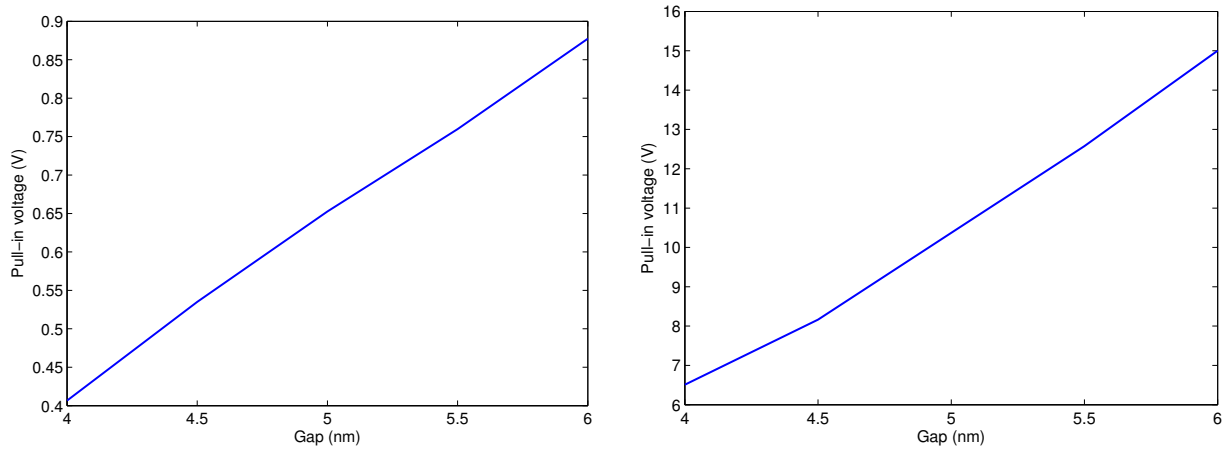
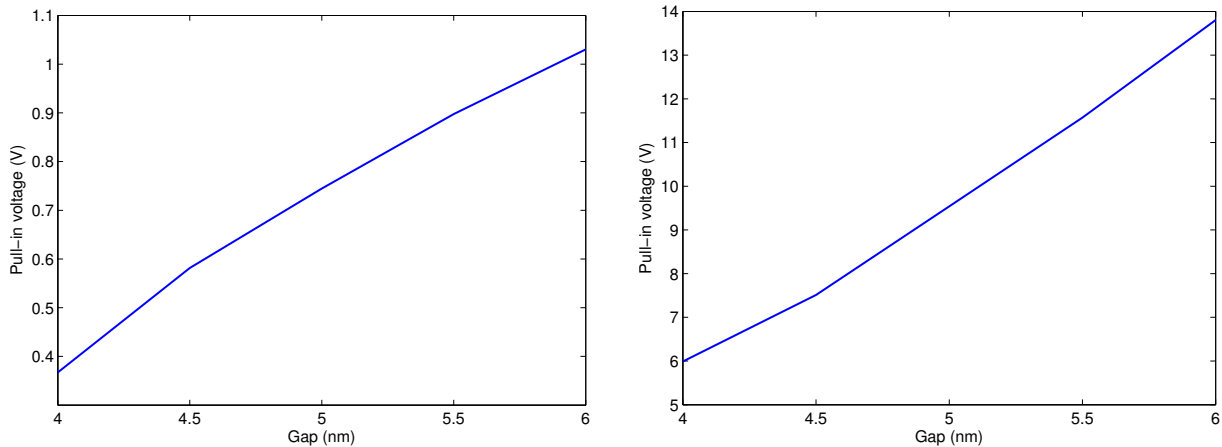**Figure 5.** Static pull-in voltages versus gap between graphene sheets for CNTs with (left) cantilever and (right) doubly clamped boundary conditions.

The effects of gap increment on the static pull-in voltages of the CNTs are depicted in Figure 5. According to this figure, an increase in the gap increases the pull-in voltages of CNTs under both boundary conditions. Similarly to having longer CNTs, smaller gaps may lead to pull-in of the CNTs without application of electrostatic actuation, that is, only due to vdW effects. In general, the variation of each parameter resulting in a weaker structure, such as increasing length or decreasing radius or gap, may increase the possibility of occurrence of pull-in.

3.2. *Vibration of CNTs under step DC voltage.* The vibration behaviors of the cantilever and doubly clamped CNTs with dimensions as reported in [Dequesnes et al. 2002] are illustrated in Figure 6. In this figure, an increment in the applied voltage results in larger vibration amplitudes. This is correct for both boundary conditions. However, the variation of natural frequency leads to different behaviors. For cantilever boundary conditions, increasing the applied voltage leads to a decrease in the natural frequency.
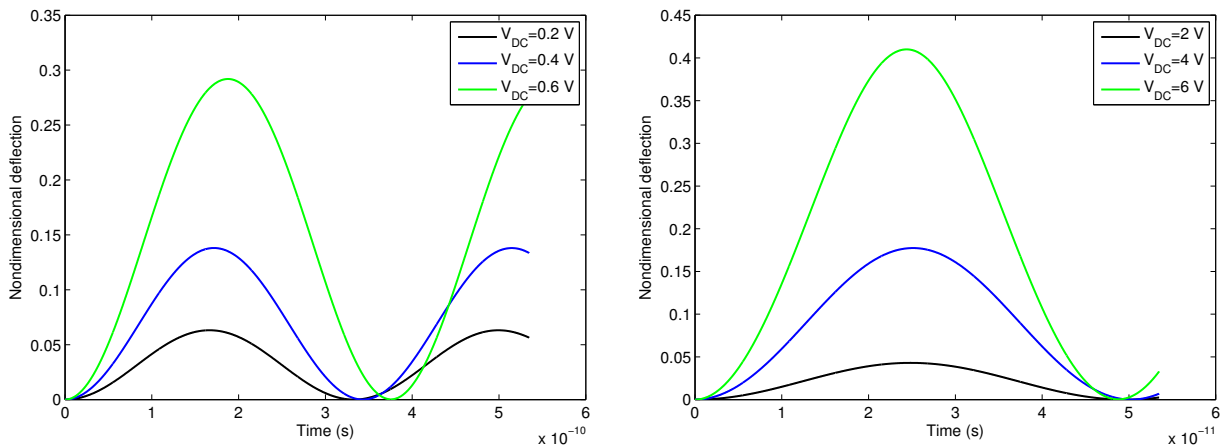
Figure 6. Vibration of CNTs with (left) cantilever and (right) doubly clamped boundary conditions under step DC voltage.

Figure 7. Dynamic pull-in voltages versus length of CNTs with (left) cantilever and (right) doubly clamped boundary conditions.

But, for the doubly clamped boundary conditions, in general, a voltage increment results in increasing frequency. Dependency of the natural frequency on the applied voltage or applied force is often a sign of a nonlinear system, because in linear systems the frequency does not depend on the applied force.

We next investigate the effects of changing the dimensions of the nanostructure on the dynamic pull-in voltages of CNTs under the boundary conditions mentioned. The physical and geometrical conditions of the CNTs studied in this subsection are same as those in the previous subsection.

Figure 7 show the variation of dynamic pull-in voltages versus length changes of CNTs under step DC voltage with cantilever and doubly clamped boundary conditions. According to this figure, we conclude that a length increment results in a decrease in dynamic pull-in voltage. However, the numerical range of variation is higher for doubly clamped boundary conditions.

Figure 8 shows the dynamic pull-in voltages versus radius increment of CNTs under step DC voltage with cantilever and doubly clamped boundary conditions. The figure reveals that, similarly to the static

Figure 8. Dynamic pull-in voltages versus radius of CNTs with (left) cantilever and (right) doubly clamped boundary conditions.

Figure 9. Dynamic pull-in voltages versus gap of CNTs with (left) cantilever and (right) doubly clamped boundary conditions.

case, the radius increment increases the dynamic pull-in voltages of CNTs with both boundary conditions. This can be attributed to the stiffer structures of CNTs with larger diameters. Comparison between the static and dynamic pull-in voltages show that the static pull-in voltages exceed the dynamic ones.

Figure 9 depicts the effects of gap increment on the dynamic pull-in voltages of CNTs with the considered boundary conditions. Based on this figure, it can be concluded that increasing the gap increases the dynamic pull-in voltages of CNTs with both boundary conditions. This fact can be attributed to weakening of the electrostatic and vdW forces with an increasing gap. Thus higher voltages should be applied to compensate for the weakening effects of increasing the gap to reach the pull-in behaviors.

4. Conclusion

This paper presents the static and dynamic deflection of carbon nanotubes (CNTs) under electrostatic actuation in the presence of vdW interactions. The homotopy perturbation method was applied to investigate the effects of diameter, length, and gap distance variations on CNTs with cantilever and doubly clamped boundary conditions. The results suggest that CNTs with longer lengths and smaller diameters were more vulnerable to pull-in. However, pull-in phenomena noticeably depended also on the gap distance between the CNT and the substrate. Smaller gaps resulted in lower pull-in voltages. Our figures suggest that decreasing the gap or increasing the length may lead to conditions in which the pull-in occurs only via vdW interaction, without electrostatic actuation. Similar investigations were conducted for nanostructures under step DC voltages and the dynamic behaviors were studied.

References

[Abadyan et al. 2010] M. Abadyan, A. Novinzadeh, and A. S. Kazemi, "Approximating the effect of the Casimir force on the instability of electrostatic nano-cantilevers", *Physica Scr.* **81**:1 (2010), Article ID #015801.

[Ansola et al. 2012] R. Ansola, E. Veguería, J. Canales, and C. Alonso, "Evolutionary optimization of compliant mechanisms subjected to non-uniform thermal effects", *Finite Elem. Anal. Des.* **57** (2012), 1–14.

[Batra et al. 2008] R. C. Batra, M. Porfiri, and D. Spinello, "Reduced-order models for microelectromechanical rectangular and circular plates incorporating the Casimir force", *Int. J. Solids Struct.* **45**:11–12 (2008), 3558–3583.

[Darvishian et al. 2012] A. Darvishian, H. Moeenfard, M. T. Ahmadian, and H. Zohoor, "A coupled two degree of freedom pull-in model for micromirrors under capillary force", *Acta Mech.* **223**:2 (2012), 387–394.

[Dequesnes et al. 2002] M. Dequesnes, S. V. Rotkin, and N. R. Aluru, "Calculation of pull-in voltages for carbon-nanotube-based nanoelectromechanical switches", *Nanotechnology* **13** (2002), 120–131.

[Jia et al. 2011] X. L. Jia, J. Yang, and S. Kitipornchai, "Pull-in instability of geometrically nonlinear micro-switches under electrostatic and Casimir forces", *Acta Mech.* **218**:1–2 (2011), 161–174.

[Kahrobaiyan et al. 2011] M. H. Kahrobaiyan, M. Rahaeifard, and M. T. Ahmadian, "Nonlinear dynamic analysis of a V-shaped microcantilever of an atomic force microscope", *Appl. Math. Model.* **35**:12 (2011), 5903–5919.

[Ke and Espinosa 2005] C. Ke and H. D. Espinosa, "Numerical analysis of nanotube-based NEMS devices, I: Electrostatic charge distribution on multiwalled nanotubes", *J. Appl. Mech.* (*ASME*) **72**:5 (2005), 721–725.

[Ke et al. 2005] C. Ke, H. D. Espinosa, and N. Pugno, "Numerical analysis of nanotube based NEMS devices, II: Role of finite kinematics, stretching and charge concentrations", *J. Appl. Mech.* (*ASME*) **72**:5 (2005), 726–731.

[Koochi et al. 2012] A. Koochi, A. S. Kazemi, F. Khandani, and M. Abadyan, "Influence of surface effects on size-dependent instability of nano-actuators in the presence of quantum vacuum fluctuations", *Physica Scr.* **85** (2012), Article ID #035804.

[Krylov et al. 2005] S. Krylov, I. Harari, and Y. Cohen, "Stabilization of electrostatically actuated microstructures using parametric excitation", *J. Micromech. Microeng.* **15**:6 (2005), 1188–1204.

[Moeenfard and Ahmadian 2012] H. Moeenfard and M. T. Ahmadian, "The influence of vertical deflection of the supports in modeling squeeze film damping in torsional micromirrors", *Microelectron. J.* **43**:8 (2012), 530–536.

[Moeenfard et al. 2012] H. Moeenfard, A. Darvishian, and M. T. Ahmaidan, "Static behavior of nano/micromirrors under the effect of Casimir force, an analytical approach", *J. Mech. Sci. Technol.* **26**:2 (2012), 537–543.

[Moghimi Zand and Ahmadian 2009] M. Moghimi Zand and M. T. Ahmadian, "Application of homotopy analysis method in studying dynamic pull-in instability of microsystems", *Mech. Res. Commun.* **36**:7 (2009), 851–858.

[Moghimi Zand et al. 2009] M. Moghimi Zand, M. T. Ahmadian, and B. Rashidian, "Semi-analytic solutions to nonlinear vibrations of microbeams under suddenly applied voltages", *J. Sound Vib.* **325**:1–2 (2009), 382–396.

[Mojahedi et al. 2010] M. Mojahedi, M. Moghimi Zand, and M. T. Ahmadian, "Static pull-in analysis of electrostatically actuated microbeams using homotopy perturbation method", *Appl. Math. Model.* **34**:4 (2010), 1032–1041.

[Mojahedi et al. 2011] M. Mojahedi, M. Moghimi Zand, M. T. Ahmadian, and M. Babaei, "Analytic solutions to the oscillatory behavior and primary resonance of electrostatically actuated microbridges", *Int. J. Struct. Stab. Dyn.* **11**:6 (2011), 1119–1137.

[Ouakad and Younis 2010] H. M. Ouakad and M. I. Younis, "Nonlinear dynamics of electrically actuated carbon nanotube resonators", *J. Comput. Nonlinear Dyn.* (*ASME*) **5**:1 (2010), Article ID #011009.

[Pirbodaghi et al. 2009] T. Pirbodaghi, M. T. Ahmadian, and M. Fesanghary, "On the homotopy analysis method for non-linear vibration of beams", *Mech. Res. Commun.* **36**:2 (2009), 143–148.

[Rahaeifard et al. 2012] M. Rahaeifard, M. H. Kahrobaiyan, M. T. Ahmadian, and K. Firoozbakhsh, "Size-dependent pull-in phenomena in nonlinear microbridges", *Int. J. Mech. Sci.* **54**:1 (2012), 306–310.

[Ramezani et al. 2008a] A. Ramezani, A. Alasty, and J. Akbari, "Analytical investigation and numerical verification of Casimir effect on electrostatic nano-cantilevers", *Microsyst. Technol.* **14**:2 (2008), 145–157.

[Ramezani et al. 2008b] A. Ramezani, A. Alasty, and J. Akbari, "Closed-form approximation and numerical validation of the influence of van der Waals force on electrostatic cantilevers at nano-scale separations", *Nanotechnology* **19**:1 (2008), Article ID #015501.

[Rezazadeh et al. 2011] G. Rezazadeh, M. Fathalilou, and M. Sadeghi, "Pull-in voltage of electrostatically-actuated microbeams in terms of lumped model pull-in voltage using novel design corrective coefficients", *Sens. Imaging Int. J.* **12**:3–4 (2011), 117–131.

[Soroush et al. 2010] R. Soroush, A. Koochi, A. S. Kazemi, A. Noghrehabadi, H. Haddadpour, and M. Abadyan, "Investigating the effect of Casimir and van der Waals attractions on the electrostatic pull-in instability of nano-actuators", *Physica Scr.* **82** (2010), Article ID #045801.

[Tayyaba et al. 2012] S. Tayyaba, N. Afzulpurkar, and M. W. Ashraf, "Simulation and design optimization of piezoelectricaly actuated valveless blood pump for hemofiltration system", *Sens. Transducers J.* **139**:4 (2012), 63–78.

[Zand 2012] M. M. Zand, "The dynamic pull-in instability and snap-through behavior of initially curved microbeams", *Mech. Adv. Mater. Struct.* **19**:6 (2012), 485–491.

[Zhang and Zhao 2006] Y. Zhang and Y. Zhao, "Numerical and analytical study on the pull-in instability of micro-structure under electrostatic loading", *Sens. Actuators A Phys.* **127**:2 (2006), 366–380.

MIR MASOUD SEYYED FAKHRABADI: msfakhrabadi@gmail.com
Karaj Branch, Islamic Azad University, Karaj, Iran

ABBAS RASTGOO: arastgo@ut.ac.ir
School of Mechanical Engineering, College of Engineering, University of Tehran, Tehran, Iran

MOHAMMAD TAGHI AHMADIAN: ahmadian@sharif.edu
Department of Mechanical Engineering, Sharif University of Technology, Tehran 11365-9567, Iran

JOURNAL OF MECHANICS OF MATERIALS AND STRUCTURES

msp.org/jomms

Founded by Charles R. Steele and Marie-Louise Steele

See msp.org/jomms for submission guidelines.